

## **Investigating the Effectiveness of a Composite Patch on Repairing Pipes Subjected to Circumferential Cracks under Combined Loadings**

Gholamreza Rashed<sup>1\*</sup>, Hadi Eskandari<sup>2</sup>, and Ardeshir Savari<sup>3</sup>

<sup>1</sup> Associate Professor, Department of Mechanical Engineering, Petroleum University of Technology, Abadan, Iran

<sup>2</sup> Associate Professor, Department of Mechanical Engineering, Petroleum University of Technology, Abadan, Iran

<sup>3</sup> M.S. Student, Department of Mechanical Engineering, Petroleum University of Technology, Abadan, Iran

*Received:* September 29, 2018; *revised:* October 22, 2018; *accepted:* November 24, 2018

---

### **Abstract**

The purpose of this study is to investigate bending moment and the axial load capacity of a pressurized pipe suffering from a through-wall circumferential crack repaired by a composite sleeve. The three-dimensional finite element method (FEM) was adopted to compute the results, and the failure assessment diagram (FAD) was employed to investigate the failure behavior of the repaired pipe. The findings revealed that, for the investigated range of applied loads and angles of the crack, the interaction of brittle and ductile failure modes is negligible. Additionally, the yield strength of the cracked pipe was considered as reference stress to achieve a conservative design. Two cases of the combined loading state consisting of internal pressure/bending moment and internal pressure/axial tensile force were investigated. Repairing the crack under combined loadings using carbon-epoxy composites was studied where the influences of various parameters, including internal pressure, crack angle, and the composite patch thickness on the capacity of the cracked pipe to withstand bending moment and axial load were included. The results indicated that the bending moment and axial load capacities of the cracked pipe depend on internal pressure, crack angle, and the composite patch thickness; nevertheless, the crack angle is the main parameter. A composite sleeve can increase both bending moment and axial load capacity of the cracked pipe, but bending moment can be increased further than axial load. Using the composite patch to repair the cracked pipe caused the bending moment capacity to improve from 14.28% to 120%. On the other hand, the composite patch raised the axial load capacity from 5.1% to 93.5%. Additionally, an increase in the composite patch thickness caused the axial load capacity to extend more than bending load capacity.

**Keywords:** Cracked Pipe, Composite Patch, Combined Loading, Circumferential Crack

---

### **1. Introduction**

With the increasing demand of hydrocarbon, the exploration and production of offshore oil and gas resources are quickly developing into deepwater and ultra-deepwater areas. Up to now, pipelines are still the most economical and effective means to transport oil and gas from deepwater wells to offshore and coastal storage equipment. The subsea pipelines unavoidably incorporate different initial geometric flaws introduced in manufacturing and various combined loadings of bending and internal pressure

---

\* Corresponding Author:

Email: [g.rashed@put.ac.ir](mailto:g.rashed@put.ac.ir)

during its construction process (Mohd et al., 2015). The transporting of oil from mudline to the surface is the principal application of pipe risers in the offshore industry (Chakrabarti and Frampton, 1982). Risers are used to withstand several kinds of mechanical loading. The internal pressure that results from the fluid content inside the riser itself is the major load applied to a riser. The tensile force is also exerted on the riser by buoyancy modules and top tensioning systems on the platform to prevent buckling and extreme bending stress due to platform movement and vortex-induced vibrations (Stanton, 2006). Pipelines subjected to combined loadings can also be found in other industries; piping pieces in power plants may undergo internal pressure, bending, and torsion loads during service (Hasegawa Li, and Osakabe, 2013). Most of pipelines in nuclear power plants tolerate combined internal pressure and bending moment because of dead-weight and seismic loads; therefore, it is necessary to use an assessment method for locally wall-thinned pipelines under combined loadings (Shim et al., 2004). Moreover, the effects of the internal pressure, thermal loads, dead loads, and geotechnical loads generate combined loading conditions on the buried pipelines, which needs to be checked (Shouman and Taheri, 2009; Achour et al., 2016). The pipelines include different types of large-diameter pipes which are used at high internal pressures. The ultimate pressure of such pipes is a significant factor in material selection, structural design, safe process, and integrity assessment (Zhu and Leis, 2012). Based on the model used to simulate the damage, studies which are currently conducted to inspect the breakdown of ductile materials are divided into two kinds of microstructural and phenomenological groups. The principal reasons for the pipeline failure are external defects and corrosion; hence, evaluation approaches are required to explain how much the recognized defects in the pipelines are dangerous and critical (Ouinan et al., 2013). Cracks may occur in the pressure vessels and cylindrical pipeline structures which are conveying gas and oil. These cracks usually develop as a result of a lack of fusion through the welding process. Such cracks may extend to hazardous dimensions and become large enough to make catastrophic structural failure during the operation of the pressure vessels and pipelines (Olsø et al., 2008; Qian, 2010). Recent researches show that the application of adhesives is a useful technique of repairing cracks in the fractured constructions by improving the fatigue life of the damaged components. It has been proven that composite patching has a significant effect on decreasing the stress intensity at the tip of cracks. When composite patches are glued to a single face or on both faces of the structure, the service life of the cracked structural components is extended (Rose et al., 1988; Atluri, 1997; Kaddouri et al., 2008).

Mohd et al. (2015) studied the residual strength features of corroded subsea pipelines under combined internal pressure and bending moment. It was noticed that internal pressure ratio significantly affects the ultimate bending moment capacity of corroded pipelines. The rise of internal pressure and corrosion depth makes the more significant value of bending moment capacity. Shim et al. (2004), using three-dimensional finite element (FE) analyses, researched a pipe with local wall thinning under internal pressure and bending moment and reported that the change of internal pressure did not importantly influence the maximum moment capacity. Miki et al. (2000) studied the effects of materials, dimensions, and geometry shape on the ultimate strength of steel pipe bends using both experiments and numerical analyses. The findings revealed that the ultimate bending angle depends on the original center angle of the pipe bend. Moreover, the ultimate strength of the pipe bend decreases by raising the internal pressure. Shouman and Taheri (2009) addressed the effectiveness of fiber-reinforced composite repair systems on the externally corroded pipelines under combined internal pressure and bending. Their results revealed that once the pipe is loaded beyond the yielding point of its material at the defect region, the composite begins to take effect, thereby carrying a significant portion of the applied pressure. Chan et al. (2014) studied the stress-strain performance of an offshore corroded pipeline riser subjected to combined internal pressure, tension, and bending. They noted that, under the combined hoop, tensile, and bending loads, the riser tends to approach failure at a much lower strain compared with when each

of these loads is applied individually. Hasegawa et al. (Hasegawa, Li, and Osakabe, 2013) focused on the behavior of plastic collapse moments of pipes with circumferential through-wall cracks subjected to combined internal pressure, torsion, and bending. Their results revealed that plastic collapse bending moments decrease by increasing torsion moments for through-wall cracked pipes. Meriem-Benziane et al. (2015) studied the performance of the composite patch for repairing longitudinal cracks in API X65 pipelines under an internal pressure. The results taken from the failure assessment diagram (FAD) indicated that the value of safety factor depends on both the crack length and pressure. Meriem-Benziane et al. (2014) investigated the crack growth of pipeline API X65 subjected to circumferential crack repaired by a bonded composite patch under an internal pressure. It was shown that the stress intensity factor of the crack tip could be reduced with a double sleeve better than with a single one. However, it is necessary to investigate the capacity of the cracked pipe repaired with a composite patch under combined loadings to distinguish significant parameters. For this purpose, this study deals with the effectiveness of a composite patch on repairing a pipe subjected to a circumferential through-wall crack under the states of a combined loading consisting of internal pressure-bending moment and internal pressure-axial tensile load.

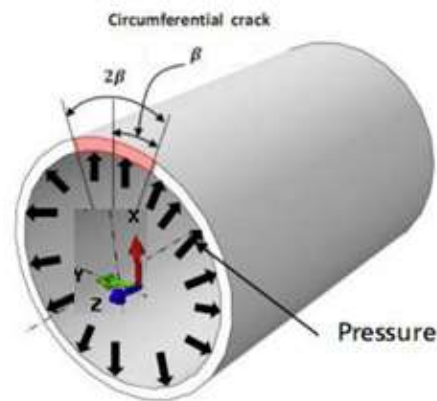
## 2. Geometrical and materials models

The geometry of the pipe subjected to a circumferential through-wall crack is displayed in Figure 1. Geometry and material properties are also tabulated in Table 1 and Table 2 respectively.

**Table 1**

Mechanical properties of the components used in the present study (Meriem-Benziane et al., 2014; Meriem-Benziane et al., 2015).

Pipeline (API X65)	Young's modulus	$E_s = 207 \text{ GPa}$
	Poisson's ratio	$\nu_s = 0.30$
Composite patch (Carbon-epoxy)	Young's modulus	$E_x = 5.5 \text{ GPa}$ $E_y = 23.4 \text{ GPa}$ $E_z = 49 \text{ GPa}$
	Shear modulus	$G_{xy} = 0.69 \text{ GPa}$ $G_{xz} = 29.6 \text{ GPa}$ $G_{yz} = 0.69 \text{ GPa}$
	Poisson's ratio	$\nu_{xy} = 0.43$ $\nu_{xz} = 0.196$ $\nu_{yz} = 0.43$
	Young's modulus	$E_a = 1.74 \text{ GPa}$
	Poisson's ratio	$\nu_a = 0.45$

**Figure 1**

Geometrical model (Meriem-Benziane et al., 2014; Meriem-Benziane et al., 2015).

**Table 1**

Geometrical properties of the components (Meriem-Benziane et al., 2014).

Component	Pipe	Adhesive (layer 1)	Sleeve (layer 1)	Adhesive (layer 2)	Sleeve (layer 2)
Inner radius (mm)	347	364.5	366	372	373.5
Thickness (mm)	17.5	1.5	6.0	1.5	6.0
Length (mm)	1000	300	300	300	300

A woven fiber reinforced polymer (FRP) based on the literature (Meriem-Benziane et al., 2014; Meriem-Benziane et al., 2015) was employed to repair the cracked pipe. Also, the fiber and polymer matrix were composed of carbon fiber and epoxy resin respectively.

### 3. Finite element model

The FE code ANSYS Workbench was used for finite element modelling. The finite element model includes a pipe with a circumferential through-wall crack, two layers of the adhesive, and two layers of a composite patch. Two layers of the elements in the thickness direction were used to construct the pipe, and one layer was employed to create adhesives and patches. The type of element used to construct the pipe structure, the adhesive layer, and the composite material was SOLID186, which is a higher order 3-D 20-node solid element exhibiting a quadratic displacement behavior (ANSYS 2017). Furthermore, the types of elements used to define the connection between the components consisted of Conta174 and Targe 170. The element shape to create the pipe, the adhesive, and the composite layers was quadratic hexahedral. Along the crack front, the 20-noded hexahedral elements were collapsed to quarter-point wedge elements to simulate the  $1/\sqrt{r}$  singularity of the stress field close to the crack front. The mesh was also refined near the crack tip area. A bonded contact was defined among the components including the pipe, the adhesive, and the patch. Figure 2 shows the overall mesh of the specimen and mesh refinement in the crack tip region. As a result of the symmetry, only one-fourth of the pipeline was studied in the analysis. The FE model was validated using the work of Meriem-Benziane et al. (2014). For this purpose, only an internal pressure was applied to the repaired pipe, and the pipeline ends were fixed. For applying the combined loadings, at the first step, an internal pressure was applied to the pipe; then, a remote point was created in the pipe end. Finally, remote displacement and bending moment were subjected to this point. To avoid rigid body motion, all the degrees of freedom, except for rotation around the  $x$ -axis and displacement in the axial direction of the pipe, were removed (Figure 3). In case of combined internal pressure-axial tension, after applying the internal pressure, the axial force was

exerted on the remote point, and all the degrees of freedom, except for the axial displacement of the pipe end, were fixed (Figure 4).

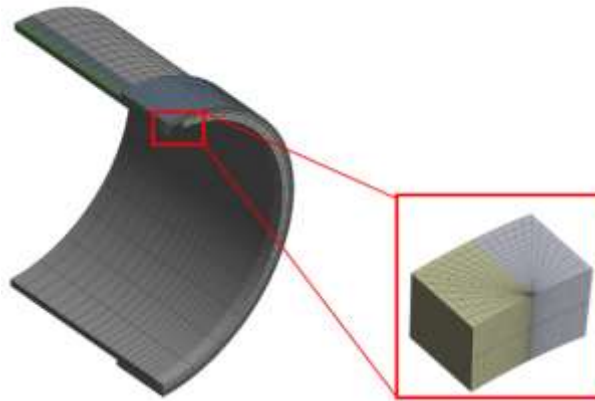


**Figure 2**

Three-dimensional finite element mesh of one-fourth of the pipe.

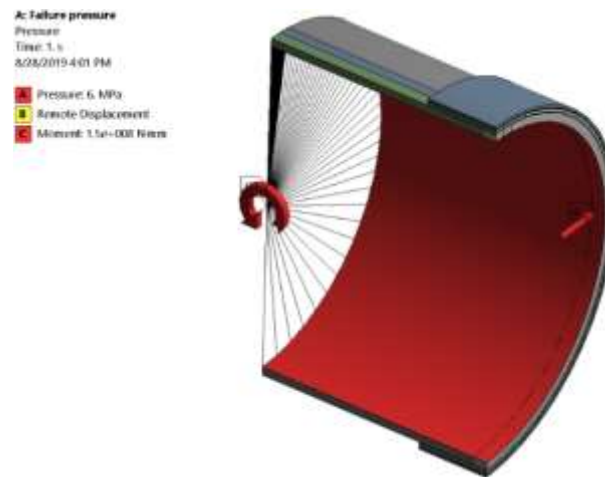


**Figure 3**

The pipe under combined internal pressure-bending moment.

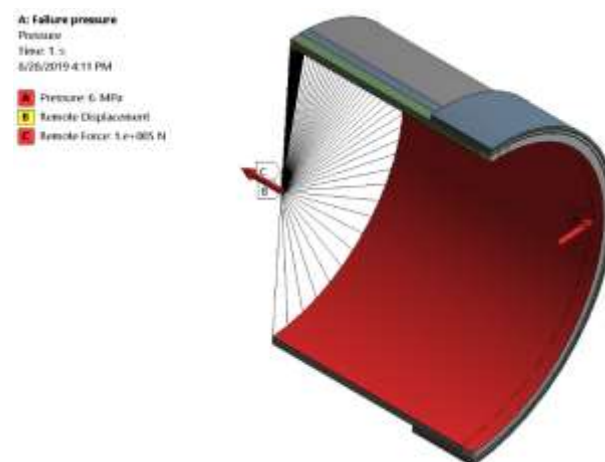


**Figure 4**

The pipe under a combined internal pressure-axial tensile load.

## 4. Results and discussion

First, the accuracy and validation of the finite element model are investigated. Then, the criterion for obtaining the bending moment and axial tensile load is introduced. Finally, the results of combined loading conditions are presented. The internal pressure applied to the pipe is up to 7.5 MPa, which is the normal service pressure for gas transmission. The results are presented in terms of  $R = P_i / 7.5$  (i.e. the ratio of the applied internal pressure to the final service pressure) as well as the crack angle.

### 4.1. Validation of the finite element model

The convergence of the finite element mesh in the case of the repaired pipe under an internal pressure at different crack angles was investigated. Comparing the results of the simulation with the result of Meriem-Benziane (Meriem-Benziane et al., 2014) showed that the highest relative error is less than 10%. The criterion for obtaining bending moment and axial load is according to the failure assessment diagram (FAD). The Structural Integrity Assessment Procedure (SINTAP) for European Industry (Duell et al., 2008; Chen and Pan, 2013) is the FAD and displays the failure curve as a critical non-dimensional SIF ( $K_r = K_I / K_{IC}$ ) versus the non-dimensional stress or loading factor ( $L_r = \sigma / \sigma_y$ ). The mathematical formulations of the FAD can be written as follows:

$$K_r = \left[ 1 + \frac{L_r^2}{2} \right]^{-0.5} \left[ 0.3 + 0.7e^{-0.6L_r^2} \right] \text{ for } 0 \leq L_r \leq 1 \quad (1)$$

$$L_r^{max} = 1 + \left( \frac{150}{\sigma_y} \right)^{2.5}$$

For the metal of API X65 pipeline:  $\sigma_y = 484.5$  MPa and  $K_{IC} = 300$  MPa $\sqrt{m}$  (Lee et al., 2004). The FAD is plotted in Figure 5 for API X65; based on this diagram, if  $K_r = 1$  and  $L_r = 1$ , the structure fails in brittle fracture and plastic collapse modes respectively. If  $0 \leq L_r, K_r \leq 1$ , collapse and fracture interact. Based on the model simulated herein, for combined loading conditions, the value of  $K_I$  was calculated up to 12.92 MPa $\sqrt{m}$ , which results in  $K_r^{max} = 0.043 \ll 1$ , but, under such a condition, stress reaches the yield strength. Therefore, the cooperation of stress and stress intensity factor can be neglected. As a result, when stress in the pipe equals the yield strength of the pipe material, failure requirement is satisfied.

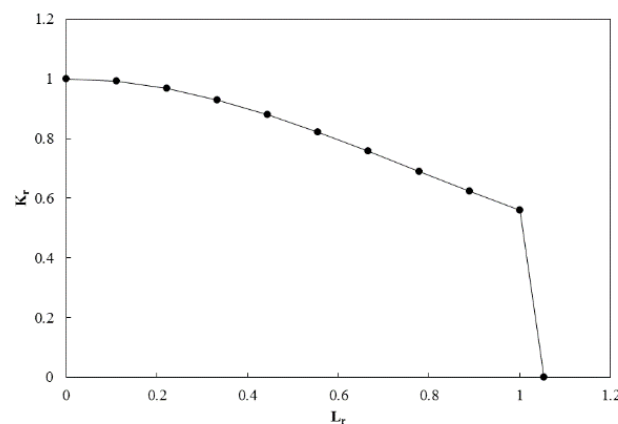


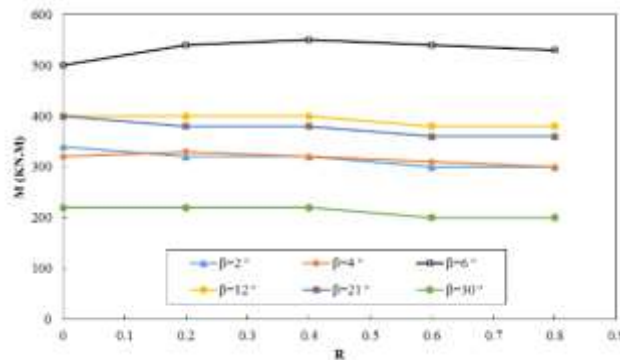
**Figure 5**

Presentation of failure assessment diagram for API X65.

## 4.2. Pipe under combined internal pressure-bending moment

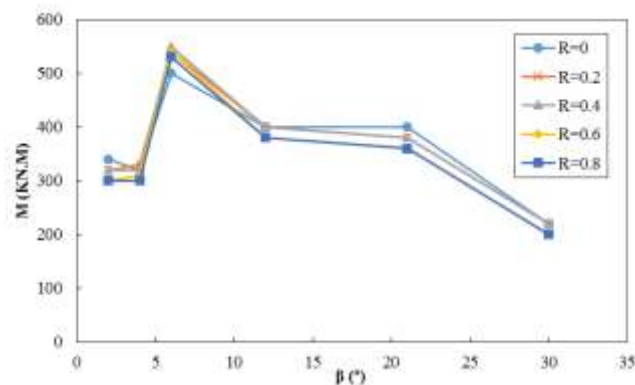
Figure 6 illustrates the bending moment capacity of the repaired pipe versus  $R$  (pressure ratio) at several crack angles. Since the pressure ratio increases, the reduction of the bending load is not significant. In Figure 7, bending capacity is exhibited versus crack angle according to the various pressure ratios. It can be seen that by increasing the crack angle from 2 to 6 degrees, the bending capacity rises; nonetheless, in the crack angle range of 6° to 30°, the bending moment diminishes. For crack angles in the range of 21° to 30°, bending moment drops at a higher rate.

Figure 8 compares bending moment capacity versus crack angle for the pipes with and without the composite patch at pressure ratios in the range of 0 to 0.8. The role of the patch in the bending moment enhancement can be recognized. The composite patch is not only able to improve the bending load capacity at different crack angles, but also able to reduce the slope of the diagrams compared to the non-repaired pipe diagrams. In the case of a crack with an angle of 30°, the bending moment of the repaired pipe has increased by 120%, which is the highest patch efficiency; the lowest efficiency is for two cases in which the pressure ratios are 0.2 and 0.4, and the crack angle is 2°. In such cases, the increase in the bending moment is 14.28%. In Figure 9, the bending moment capacity versus pressure ratio at different crack angles for the pipes with and without the composite patch are compared. By increasing the crack angle, the role of the patch in tolerating the load enhances. In fact, by increasing crack angle, although the integrity of the pipe is reduced, the loads are better transmitted to the patch. However, in general, raising crack angle in the range of 6° to 30° causes the bending moment capacity of the pipe to fall.



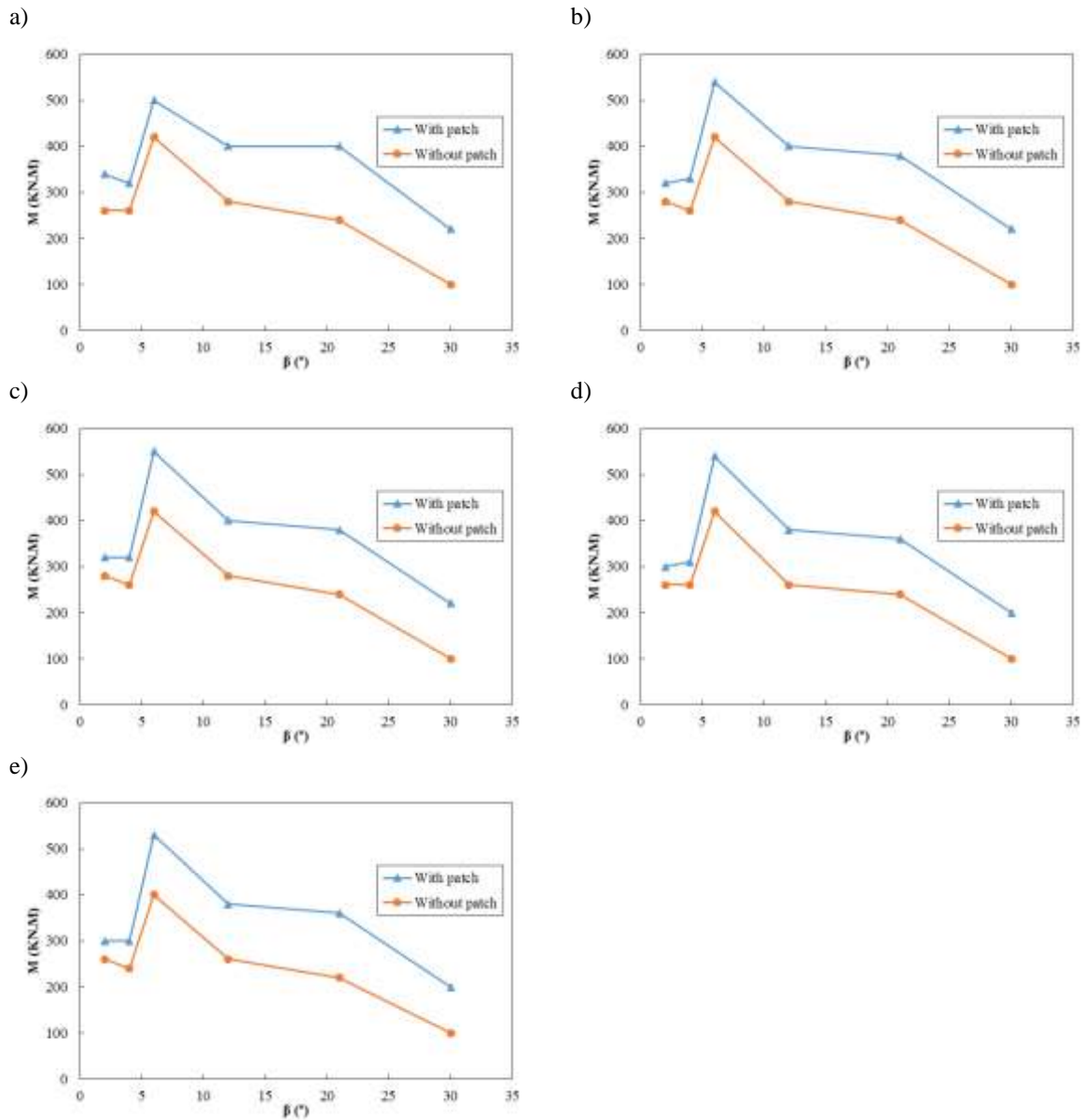
**Figure 6**

The bending moment capacity of the pipe versus pressure ratio at different crack angles.



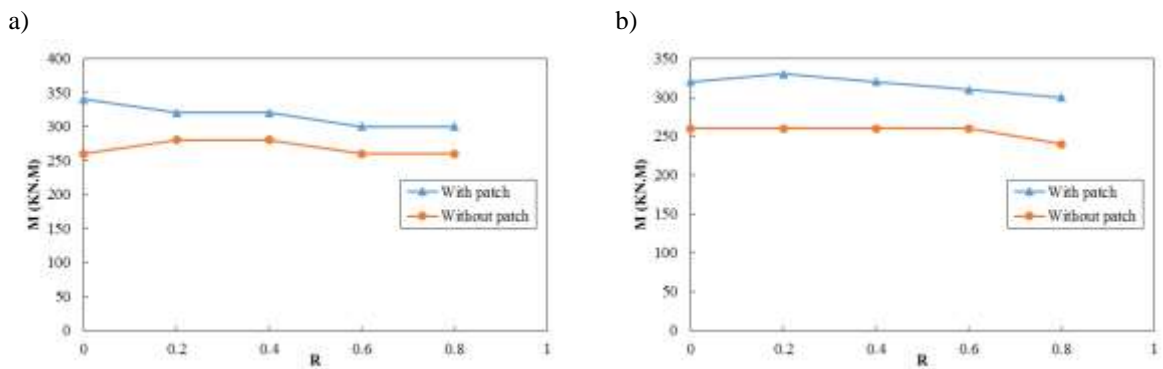
**Figure 7**

The bending moment capacity of the pipe versus crack angle at different pressure ratios.



**Figure 8**

Comparison of bending moment capacity versus crack angle for the pipes with and without the composite patch at various pressure ratios, including a)  $R=0$ , b)  $R=0.2$ , c)  $R=0.4$ , d)  $R=0.6$ , and e)  $R=0.8$ .



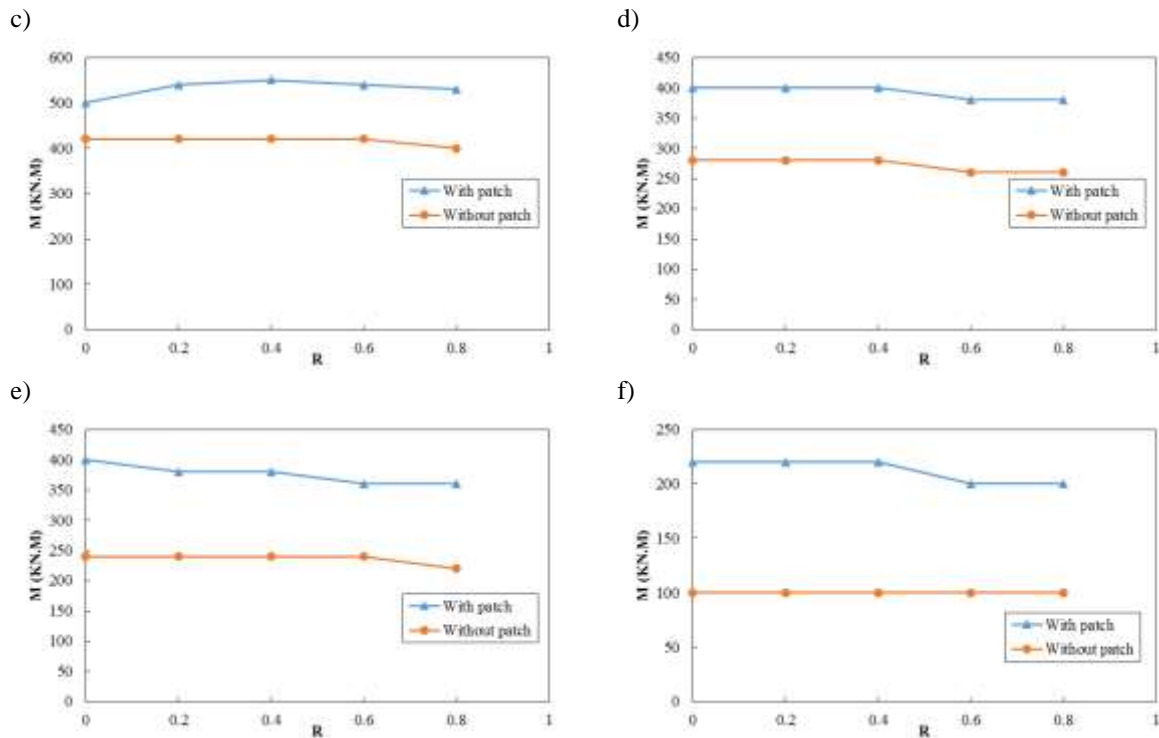
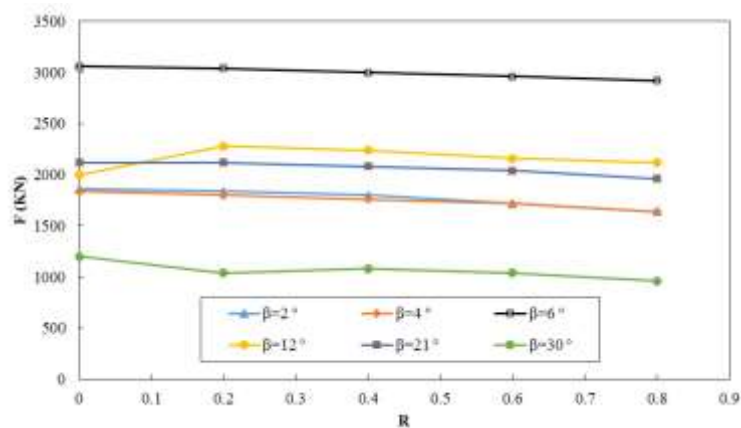


**Figure 9**

Comparison of bending moment capacity versus pressure ratio for the pipes with and without the patch at different crack angles, including a)  $\beta=2^\circ$ , b)  $\beta=4^\circ$ , c)  $\beta=6^\circ$ , d)  $\beta=12^\circ$ , e)  $\beta=21^\circ$ , and f)  $\beta=30^\circ$ .

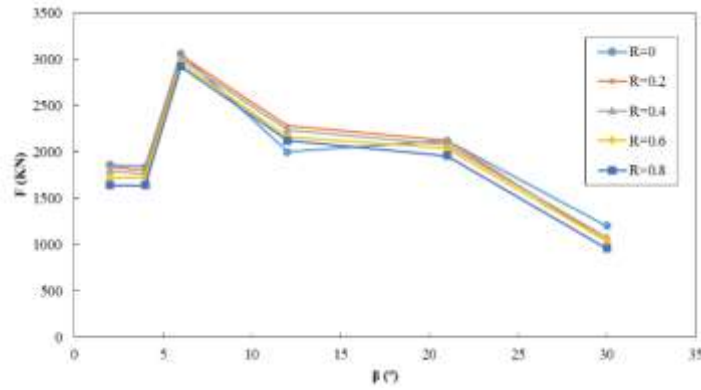
### 4.3. Pipe under a combined internal pressure-axial tensile load

The tension load capacity of the repaired pipe versus pressure ratio can be seen in Figure 10. The higher the pressure ratio is, the lower the axial load becomes; however, its reduction is negligible. Figure 11 depicts the axial load versus crack angle; the highest axial force capacity is 3060 kN which occurs when the crack angle and pressure ratio are  $6^\circ$  and 0 respectively. The lowest load is 960 kN for a case in which the crack angle and pressure ratio are  $30^\circ$  and 0.8 respectively. It is observed that when crack angle increases in the range of  $21^\circ$  to  $30^\circ$ , axial load experiences a significant reduction.



**Figure 10**

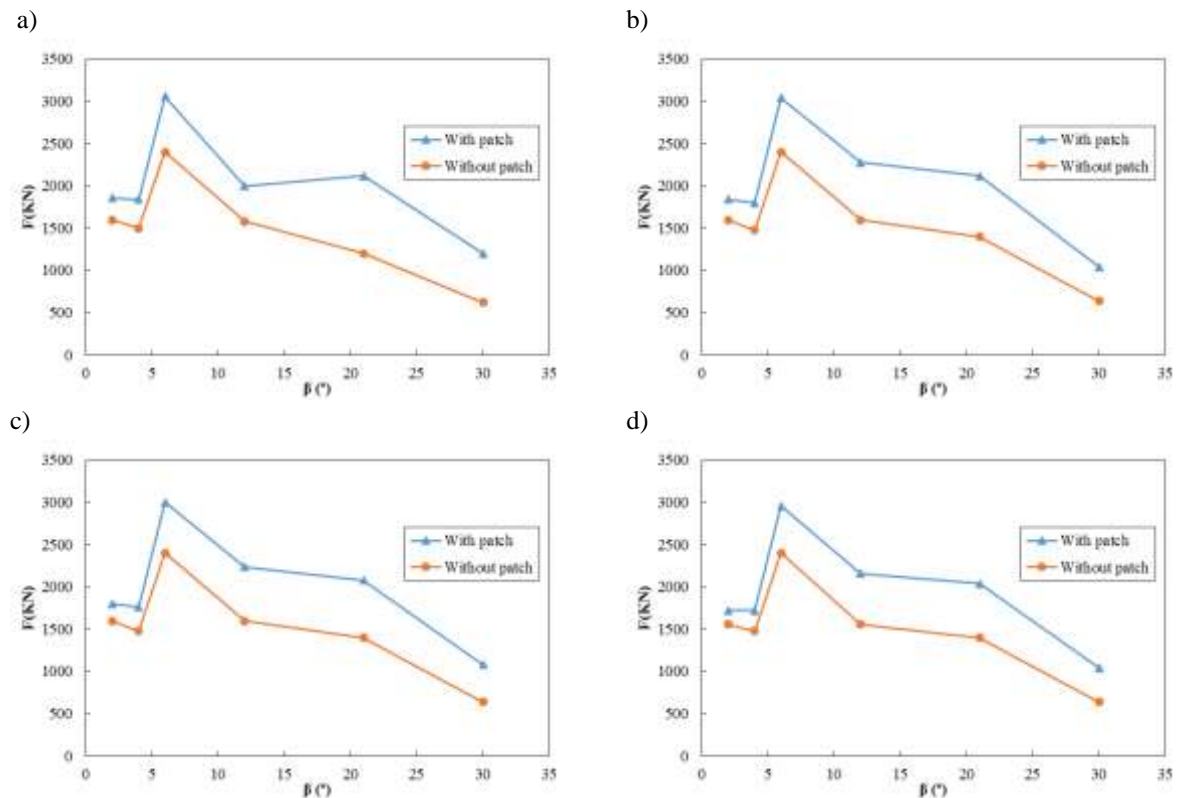
The axial tensile load capacity of the pipe versus pressure ratio at different crack angles.



**Figure 11**

The axial tensile load capacity of the pipe versus crack angles at different pressure ratios.

Figure 12 compares the axial load capacity of the repaired and non-repaired pipes at various pressure ratios. It can be seen that the composite sleeve can improve the load capacity in all the cases. The highest patch effectiveness is 93.5% which occurs for the case in which  $R=0$  and  $\beta=30^\circ$ . In contrast, when  $R=0.8$  and  $\beta=2^\circ$ , the composite patch is only able to reinforce the cracked pipe by 5.1%. It can be observed that the higher the pressure is, the lower the axial load capacity of the pipe becomes. The axial force capacity of the repaired and non-repaired pipes at various crack angles can be seen in Figure 13. By increasing crack angle, axial load versus pressure ratio does not indicate a significant reduction. However, the repaired pipe capacity diminishes more than the non-repaired one.



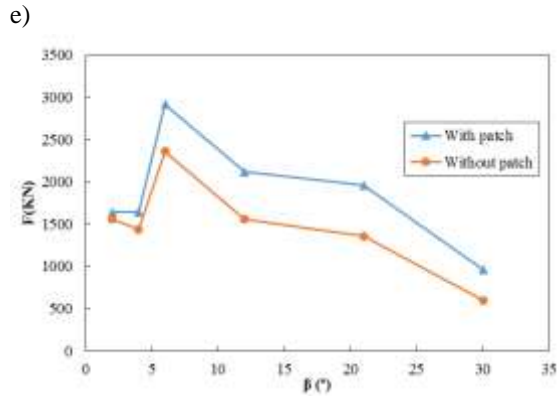


**Figure 12**

Comparison of axial load capacity versus crack angle for the pipes with and without the composite patch at various pressure ratios, including a)  $R=0$ , b)  $R=0.2$ , c)  $R=0.4$ , d)  $R=0.6$ , and e)  $R=0.8$ .

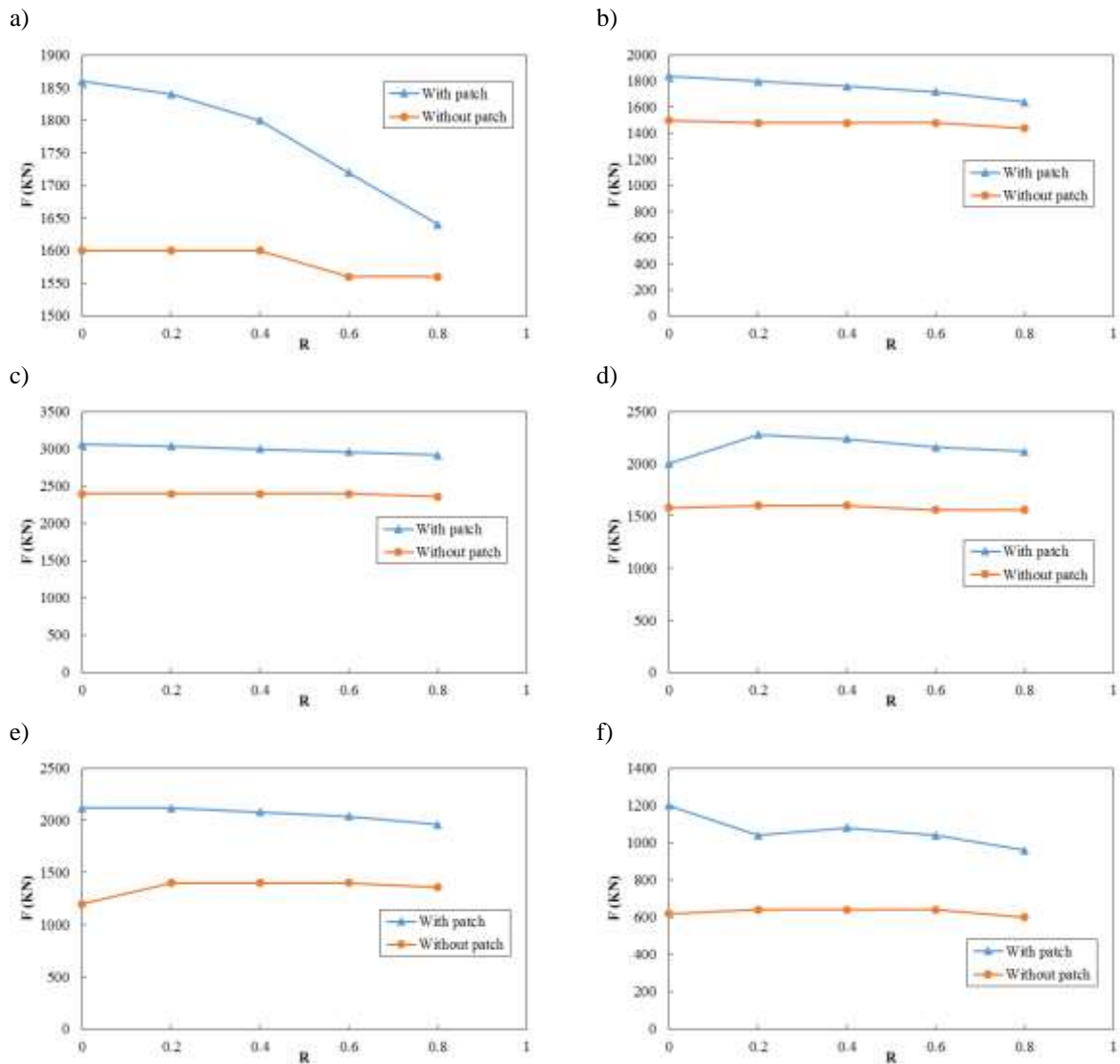


**Figure 13**

Comparison of axial load capacity versus pressure ratio for the pipes with and without the composite patch at different crack angles, including a)  $\beta=2^\circ$ , b)  $\beta=4^\circ$ , c)  $\beta=6^\circ$ , d)  $\beta=12^\circ$ , e)  $\beta=21^\circ$ , and f)  $\beta=30^\circ$ .

#### 4.4. Effect of the patch thickness on the bending and axial load capacities

To investigate the effect of the patch thickness on the pipe load capacity, at three crack angles of  $2^\circ$ ,  $12^\circ$ , and  $30^\circ$ , the pressure ratio of 0.8 was investigated (Figure 14 and Figure 15). In these two diagrams,  $n = t/t_0$  and  $t_0$  is the initial thickness of the patch presented in Table 2. By increasing the thickness of the composite patch, the bending moment capacity of the pipe at  $\beta=2^\circ$ ,  $12^\circ$ , and  $30^\circ$  increased by 3.3, 7.8, and 17 % respectively. On the other hand, the corresponding increase in the axial load capacity was 3.6, 3.8, and 35.4%. Therefore, by increasing the crack angle, the effect of the patch thickness on improving the axial load capacity, compared to the bending moment, is more significant.

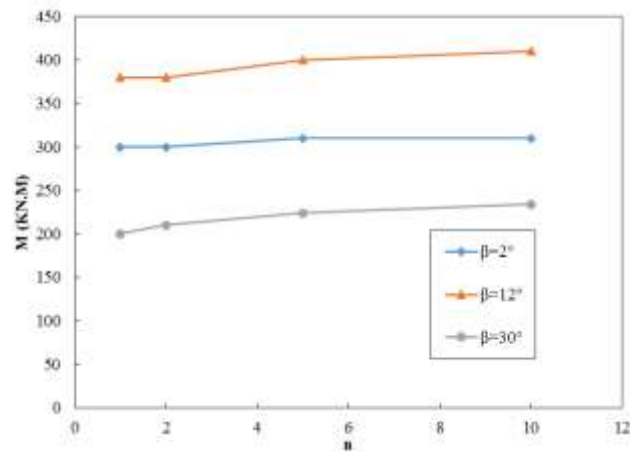


**Figure 14**

Influence of the patch thickness on the bending load capacity of the repaired pipe.

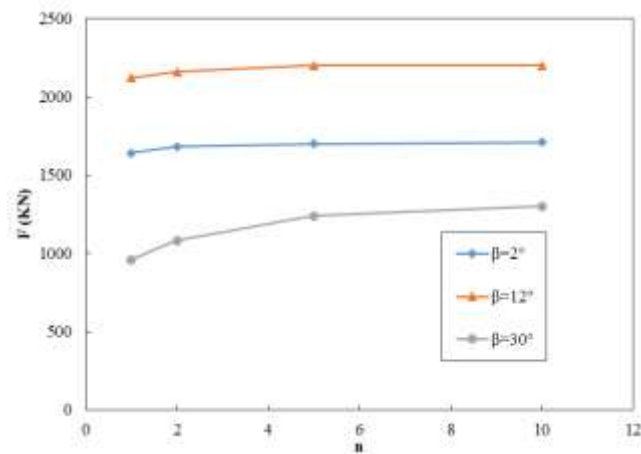


**Figure 15**

Influence of the patch thickness on the axial load capacity of the repaired pipe.

## 5. Conclusions

This study coped with the efficiency of the composite patch on repairing a pipe subjected to a through-wall circumferential crack under combined loadings, including internal pressure-bending moment and internal pressure-axial force. To this end, a three-dimensional finite element method was employed, and the commercial FE code, ANSYS Workbench, was used to analyze pipe models. The results revealed that the composite patch can increase the load capacity of the pipe in both loading conditions, but it improves bending moment capacity more than axial tensile load. The parametric studies using internal

pressure, crack angle, and patch thickness as significant variables were employed, and their effects on the load capacity of the pipe were studied. It was found out that load capacity depends on all the parameters, but the crack angle is the significant one. On the one hand, in the case where the crack angle is small, the patch performance is weak for increasing the loads. On the other hand, when the pipe is under either pure bending or tension, the patch is more able to sustain the loads. Repairing the cracked pipe by a composite patch resulted in improving the bending moment capacity in the range of 14.28 to 120%. Furthermore, the composite patch raised the axial load capacity in the range of 5.1 to 93.5%. Furthermore, increasing the thickness of the composite patch caused the axial load capacity to enhance more than bending moment.

Although the relations of combined loading capacity for a cracked pipe can be found in the literature (Anderson, 2017), unfortunately, the theoretical expressions of the combined loading for a cracked pipe repaired by a composite sleeve cannot easily be obtained. In fact, because of the significant number of parameters affecting the behavior of a repaired crack, it is difficult to derive an analytical formula for a repaired pipe under a combined loading. In such a field, the finite element analysis is usually employed to overcome the limitations of the analytical methods. Some researchers have tried to extract a semi-analytical formula from finite element findings; for example, Chen et al. (2013) obtained a semi-analytical formula to calculate the stress intensity factor along the crack tip for a pressurized pipe subjected to a semi-elliptical crack which is repaired by a composite patch. Therefore, extracting a semi-analytical formula to predict either the bending moment or the axial load capacity of a pressurized pipe suffering from a through-wall circumferential crack can be conducted in the future studies.

## Nomenclature

$\beta$	Crack angle
$\sigma$	Stress tensor
$K_I, K_{II}, K_{III}$	Modes I, II, and III of stress intensity factors
FAD	Failure assessment diagram
FE	Finite element
$K_r$	Non-dimensional stress intensity factor
$L_r$	Non-dimensional stress or loading factor
$R$	Pressure ratio
SINTAP	Structural integrity assessment procedure

## References

- Achour, A., Abdulmohsen A., Faycal B., Bel A. Bachir B., and Djamel O., Analysis of Repaired Cracks with Bonded Composite Wrap in Pipes under Bending, *Journal of Pressure Vessel Technology*, Vol. 138, No. 6, p. 060909, 2016.
- Anderson, T. L., *Fracture Mechanics, Fundamentals and Applications*, CRC Press, 2017.
- ANSYS, *ANSYS Software and User Manual*, ANSYS Inc., 2017.
- Atluri, S. N., *Structural Integrity and Durability*, Tech Science Press, 1997.
- Chakrabarti, S. K. and Frampton, R. E., Review of Riser Analysis Techniques, *Applied Ocean Research*, Vol. 4, No. 2, p. 73-90, 1982.

- Chan, P., Tshai, K., Johnson, M., and Li, S., Finite Element Analysis of Combined Static Loadings on Offshore Pipe Riser Repaired with Fiber-reinforced Composite Laminates, *Journal of Reinforced Plastics and Composites*, Vol. 33, No. 6, p. 514-525, 2014.
- Chen, J. and Pan, H., Stress Intensity Factor of Semi-elliptical Surface Crack in a Cylinder with Hoop Wrapped Composite Layer, *International Journal of Pressure Vessels and Piping*, Vol. 110, p. 77-81, 2013.
- Duell, J., Wilson, J., and Kessler, M., Analysis of a Carbon Composite Overwrap Pipeline Repair System, *International Journal of Pressure Vessels and Piping*, Vol. 85, No. 11, p. 782-788, 2008.
- Hasegawa, K., Li, Y., and Osakabe, K., Combined Torsion and Bending Moments at Collapse for Pipes with Circumferentially Through-wall Crack, Paper Presented at The ICMFF10, 2013
- Kaddouri, K., Ouinas, D., and Bouiadjra, B. B., FE Analysis of The Behavior of Octagonal Bonded Composite Repair in Aircraft Structures, *Computational Materials Science*, Vol. 43, No. 4, p. 1109-1111, 2008.
- Lee, J. S., Ju, J. B., Jang, J. I., Kim, W. S., and Kwon, D. , Weld Crack Assessments in API X65 Pipeline: Failure Assessment Diagrams with Variations in Representative Mechanical Properties, *Materials Science and Engineering: A*, Vol. 373, No. 1-2, p. 122-130, 2004.
- Meriem-Benziane, M., Abdul-Wahab, S. A., Merah, N., and Babaziane, B., Numerical Analysis of the Performances of Bonded Composite Repair with Adhesive Band in Pipeline API X65, Paper Presented at the Advanced Materials Research, 2014.
- Meriem-Benziane, M., Abdul-Wahab, S. A., Zhloul, H., Babaziane, B., Hadj-Meliani, M., and Pluinage, G., Finite Element Analysis of the Integrity of an API X65 Pipeline with a Longitudinal Crack Repaired with Single-and Double-bonded Composites, *Composites Part B: Engineering*, Vol. 77, p. 431-439, 2015.
- Miki, C., Kobayashi, T., Oguchi, N., Uchida, T., Suganuma, A., and Katoh, A., Deformation and Fracture Properties of Steel Pipe Bend with Internal Pressure Subjected to In-plane Bending, Paper Presented at the Proceedings of the 12<sup>th</sup> World Conference of Earthquake Engineering. 2000.
- Mohd, M. H., Lee, B. J., Cui, Y., and Paik, J. K., Residual Strength of Corroded Subsea Pipelines Subject to Combined Internal Pressure and Bending Moment, *Ships and Offshore Structures*, Vol. 10, No. 5, p. 554-564, 2015.
- Olsø, E., Nyhus, B., Østby, E., Berg, E., Holthe, K., Skallerud, B., and Thaulow, C., Effect of Embedded Defects in Pipelines Subjected to Plastic Strains during Operation, Paper Presented at the 18<sup>th</sup> International Offshore and Polar Engineering Conference, 2008.
- Ouinas, D., Achour, B., Bouiadjra, B. B., and Taghezout, N., The Optimization Thickness of Single/Double Composite Patch on the Stress Intensity Factor Reduction, *Journal of Reinforced Plastics and Composites*, Vol. 32, No. 9, p. 654-663, 2013.
- Qian, X., K.I.T., Estimation for Embedded Flaws in Pipes Part II: Circumferentially Oriented Cracks, *International Journal of Pressure Vessels and Piping*, Vol. 87, No. 4, p. 150-164, 2010.
- Rose, L., Baker, A., and Jones, R., Bonded Repair of Aircraft Structures, Chapter Five AA Baker, R. Jones (Editions), *Theoretical Analysis of Crack Patching*, Martinus Nijhoff Publishers, p. 81-82, 1988.
- Shim, D. J., Choi, J. B., and Kim, Y. J., Failure Strength Assessment of Pipes with Local Wall Thinning Under Combined Loading Based on Finite Element Analyses, *Journal of Pressure Vessel Technology*, Vol. 126, No. 2, p. 179-183, 2004.

- Shouman, A. and Taheri, F., An Investigation into the Behavior of Composite Repaired Pipelines under Combined Internal Pressure and Bending, Paper Presented at The ASME 2009 28<sup>th</sup> International Conference on Ocean, Offshore and Arctic Engineering, 2009.
- Stanton, P., Overview of Deepwater Drilling and Production Risers, in: Technip, 2006.
- Zhu, X. K. and Leis, B. N., Evaluation of Burst Pressure Prediction Models for Line Pipes, *International Journal of Pressure Vessels and Piping*, Vol. 89, p. 85-97, 2012.